Educator Scholarship                                    Chemistry and Biochemistry

11-7-2003

# Specific Isotopic Labeling and Photooxidation-linked Structural Changes in the Manganese-stabilizing Subunit of Photosystem II

Roseann K. Sachs
*Messiah University*, rsachs@messiah.edu

Kelly M. Halverson
*University of Minnesota Twin Cities*

Bridgette A. Barry
*University of Minnesota Twin Cities*

Follow this and additional works at: https://mosaic.messiah.edu/chem_ed

Permanent URL: https://mosaic.messiah.edu/chem_ed/20

Sharpening Intellect | Deepening Christian Faith | Inspiring Action

Messiah University is a Christian university of the liberal and applied arts and sciences. Our mission is to educate men and women toward maturity of intellect, character and Christian faith in preparation for lives of service, leadership and reconciliation in church and society.

www.Messiah.edu                                    One University Ave. | Mechanicsburg PA 17055

# Specific Isotopic Labeling and Photooxidation-linked Structural Changes in the Manganese-stabilizing Subunit of Photosystem II*

**Roseann K. Sachs‡§¶, Kelly M. Halverson‡∥, and Bridgette A. Barry‡\*\***

*From the ‡Department of Biochemistry, Molecular Biology, and Biophysics, University of Minnesota,
St. Paul, Minnesota 55108 and the §Department of Chemistry, Colorado College, Colorado Springs, Colorado 80903*

Photosystem II (PSII) oxidizes water to molecular oxygen; the catalytic site is a cluster of four manganese ions. The catalytic site undergoes four sequential light-driven oxidation steps to form oxygen; these sequentially oxidized states are referred to as the $S_n$ states, where $n$ refers to the number of oxidizing equivalents stored. The extrinsic manganese stabilizing protein (MSP) of PSII influences the efficiency and stability of the manganese cluster, as well as the rates of the S state transitions. To understand how MSP influences photosynthetic water oxidation, we have employed isotope editing and difference Fourier transform infrared spectroscopy. MSP was expressed in *Escherichia coli* under conditions in which MSP aspartic and glutamic acid residues label at yields of 65 and 41%, respectively. Asparagine and glutamine were also labeled by this approach. GC/MS analysis was consistent with minimal scrambling of label into other amino acid residues and with no significant scrambling into the peptide bond. Selectively labeled MSP was then reconstituted to PSII, which had been stripped of native MSP. Difference Fourier transform infrared spectroscopy was used to probe the $S_1Q_A$ to $S_2Q_A^-$ transition at 200 K, as well as the $S_1Q_B$ to $S_2Q_B^-$ transition at 277 K. These experiments show that aspargine, glutamine, and glutamate residues in MSP are perturbed by photooxidation of manganese during the $S_1$ to $S_2$ transition.

Photosystem II (PSII)[1] is the multisubunit membrane protein responsible for the light-driven oxidation of water to molecular oxygen in higher plants, algae, and cyanobacteria (1). PSII contains multiple protein subunits, most of which are hydrophobic and traverse the membrane. Intrinsic PSII proteins ligate the antenna and the reaction center chlorophylls, as well as other cofactors that take part in the oxidation/reduction reactions (2). These intrinsic subunits include the chlorophyll *a*-binding proteins, CP47 and CP43, the $\alpha$ and $\beta$ subunits of cytochrome $b_{559}$, and the polypeptides known as D1 and D2. D1 and D2 form the heterodimeric core of PSII (3–5).

The catalytic site of the oxygen-evolving complex contains a cluster of four manganese atoms. As water is oxidized, the manganese cluster cycles through five oxidation states, called the $S_n$ states (6). Water oxidation is initiated by excitation of the primary chlorophyll donor, $P_{680}$. $P_{680}^*$ transfers an electron to pheophytin, which in turn reduces a bound plastoquinone, called $Q_A$. $Q_A^-$ reduces a second quinone, $Q_B$. $Q_B$ acts as a two-electron and two-proton acceptor. On the donor side of PSII, $P_{680}^+$ oxidizes a redox active tyrosine, Z, which in turn oxidizes the catalytic site. Redox tyrosine $Y_D$ and a chlorophyll, $Chl_Z$, are alternate electron donors to $P_{680}^+$. Four sequential photooxidations are required for oxygen production (reviewed in Ref. 1).

PSII contains several extrinsic subunits, which are bound to the inner lumenal surface of the reaction center (reviewed in Ref. 7). The extrinsic subunits of PSII play key roles in enzymatic activity and stability, but the mechanism of these effects is still unknown. The largest extrinsic subunit is called the manganese stabilizing protein (MSP), and this subunit is found in plants, cyanobacteria, and eukaryotic algae. MSP can be removed from the reaction center with high concentrations of $CaCl_2$ or with low concentrations of urea (8, 9). After its removal by these methods, the steady-state rate of oxygen evolution is decreased, and two manganese atoms are easily lost as $Mn^{2+}$ (10). Loss of manganese inactivates the enzyme; these MSP-dependent deactivation reactions can be prevented by addition of high concentrations of chloride to the preparation (10, 11). An *Escherichia coli*-expressed version of spinach MSP is able to functionally reconstitute oxygen evolution in spinach PSII, from which the native subunit has been removed (12, 13).

MSP exhibits anomalous migration on SDS-PAGE and size exclusion chromatography (see Ref. 14 and references therein). Both hydrodynamic (15) and small-angle x-ray scattering experiments (16) suggest that MSP is a prolate ellipsoid in solution. Axial ratios of 4.2 (15) and 4.8 (16) have been reported. Both CD and FT-IR analysis suggest that MSP is primarily a $\beta$ sheet protein (17–21). However, FT-IR studies of MSP in solution have suggested some variability in its secondary structure content (19, 21), as have protein mapping studies of MSP from different organisms (22). These results, as well as the high temperature stability of MSP, have been explained by the suggestion that MSP is an intrinsically disordered protein and that this intrinsic disorder is important in facilitating assembly (19).

Because MSP can be removed from PSII, expressed in *E. coli*, and then reconstituted to the enzyme, isotope editing was employed to study its functional role in PSII (21, 23). MSP was isotopically edited via expression in an *E. coli* strain grown on

¶ Permanent address: Dept. of Chemistry and Biochemistry, Messiah College, One College Ave., Grantham, PA 17027.

∥ Present address: Bacteriology Division, United States Army Medical Research Inst. of Infectious Diseases, 1425 Porter St., Ft. Detrick, MD 21702.

\*\* To whom correspondence should be addressed: School of Chemistry and Biochemistry, Georgia Institute of Technology, Atlanta, GA 30332. E-mail: barry@cbs.umn.edu.

[1] The abbreviations used are: PSII, photosystem II; Chl, chlorophyll; DCMU, 3-(3,4-dichlorophenyl)-1,1-dimethylurea; FT-IR, Fourier transform infrared; GC/MS, gas chromatography/mass spectrometry; MES, 2-(*N*-morpholino)ethanesulfonic acid; MSP, manganese stabilizing protein.

$^{13}$C-labeled glucose. $^{13}$C-Labeled MSP was purified and bound to PSII. As the only $^{13}$C-labeled PSII subunit, MSP could then be detected with vibrational spectroscopy, which is sensitive to isotopic composition. Using this approach, FT-IR experiments showed that a substantial change in MSP secondary structure occurred with reconstitution (21). This result is in agreement with cross-linking studies, which also suggest a change in MSP structure upon PSII binding (24).

Difference FT-IR spectroscopy and isotope editing were also employed to identify MSP structural changes that occur during the $S_1$ to $S_2$ transition (23). At 200 K, all transitions in the PSII photocycle are blocked, except the $S_1$ to $S_2$ transition, and electron transfer from $Q_A$ to $Q_B$ is also inhibited (see Ref. 25 and references therein). When glycerol-containing PSII is illuminated, the multiline form of the $S_2$ state is generated from the dark-stable $S_1$ state (26, 27). This S state transition corresponds to a manganese oxidation reaction (see Ref. 28 and references therein). Thus, it is possible to obtain a $S_2Q_A^-$-minus-$S_1Q_A$ FT-IR spectrum at 200 K by continuous illumination (see Ref. 29 and references therein). A different $S_2Q_A^-$-minus-$S_1Q_A$ FT-IR spectrum was obtained by laser flash illumination (see Refs. 30–33 and references therein). Possible reasons for these spectral differences have been discussed (34–36). A $S_2Q_B^-$-minus-$S_1Q_B$ spectrum has also been reported (36, 37).

In our previous work, $S_2Q_A^-$-minus-$S_1Q_A$ data were acquired under continuous illumination from natural abundance $^{12}$C-MSP- and $^{13}$C-MSP-reconstituted PSII. A comparison was performed by construction of a double difference, isotope-edited spectrum at 200 K (23). That analysis led to the conclusion that one or more carboxylic acid side chains in MSP contribute to the isotope-edited spectrum (23). These assignments were substantiated by comparison to $^{13}$C-labeled model compounds. Thus, it was concluded that one or more aspartic or glutamic acid residues deprotonate upon conversion of the $S_1$ state to the $S_2$ state.

To acquire more information about the role of amino acid residues in MSP, this article reports selective $^{13}$C labeling of aspartic acid/asparagine or glutamic acid/glutamine. GC/MS analysis of labeled MSP was consistent with little scrambling of label into other amino acid residues. Selectively labeled MSP was then reconstituted to PSII, and difference FT-IR spectroscopy was used to probe the $S_1$ to $S_2$ transition at two different temperatures, with both continuous and flash illumination. These experiments show that aspargine, glutamine, and glutamate residues in MSP are perturbed by photooxidation of manganese.

<div align="center">MATERIALS AND METHODS</div>

*Labeling and Purification of MSP*—Selective labeling either of aspartic acid/asparagine or glutamine/glutamic acid residues in MSP was performed via expression in *E. coli*. MSP was produced from a *psbO*-containing expression plasmid by induction with isopropyl-1-thio-β-D-galactopyranoside, as previously described (21, 23). The host strain for expression was a non-auxotropic strain, BL21(DE3) pLysS(F$^-$ *ompT* $r_B^-$ *mB*$^-$). Selective labeling was obtained by growth in a defined media, containing an excess of the $^{13}$C-labeled amino acid of choice. This media contained the following components per liter (38): 0.5 g of $MgSO_4$, 13.2 mg of $CaCl_2 \cdot 2H_2O$, 5 mg of $FeSO_4 \cdot 7H_2O$, 50 mg of nicotinic acid, 50 mg of thiamin, 2 g of sodium acetate, 1 g of ammonium chloride, 10 g of potassium phosphate dibasic, 2 g of succinic acid, 400 mg of alanine, 400 mg of glutamine, 125 mg of guanosine, 125 mg of uracil, 125 mg of cytosine, 50 mg of thymine, 400 mg of arginine, 50 mg of cystine, 400 mg of glycine, 135 mg of histidine-HCl-H$_2$O, 100 mg of isoleucine, 100 mg of leucine, 100 mg of lysine, 250 mg of methionine, 100 mg of proline, 1.6 g of serine, 200 mg of threonine, 50 mg of tryptophan, 100 mg of tyrosine, 100 mg of valine, 50 mg of phenylalanine, and 0.1 mg of biotin. For the selective $^{13}$C labeling of aspartic acid/asparagine residues in MSP, 500 mg of L-[4-$^{13}$C]aspartic acid (Isotec, 99% $^{13}$C) were added to 1 liter of the media, along with 800 mg of glutamic acid. For the selective labeling of glutamic acid/glutamine residues in MSP, 800 mg of L-[5-$^{13}$C]glutamic

acid (Isotec, 99% $^{13}$C), along with 250 mg of aspartic acid, were added to 1 liter of media. After gentle heating to dissolve all the reagents, the media was filter sterilized.

To each liter of sterilized defined media was added 10 ml of 20% glucose (for a final concentration of 0.2%), 1 ml of chloramphenicol (25 mg/ml), and 1 ml of ampicillin (50 mg/ml). One-hundred milliliters of this media was inoculated and incubated overnight at 37 °C in a rotary shaker. The following morning, 20 ml of the cell culture was added to the remaining media, and the 37 °C incubation continued until the $A_{600}$ was ~0.5. This took about 3 h. At this time, 0.2 ml of 0.2 M isopropyl-1-thio-β-D-galactopyranoside was added to induce MSP production. In addition, a 100-ml solution of 10% lactose was added; lactose was found to improve the labeling efficiency (39). After induction, the cells were grown for an additional 4 h and harvested. Natural abundance and globally $^{13}$C-labeled MSP were prepared by expression in minimal media, containing either 0.2% $^{12}$C- or 0.2% [$^{13}$C]glucose as the carbon source, as described (21). Inclusion bodies, containing MSP, were isolated, and MSP was solubilized and purified by previously described methods (21, 40).

Isotope incorporation into MSP was measured using previously employed procedures (21, 23, 41). Briefly, the protein was hydrolyzed under anaerobic conditions (42). The resulting amino acids were derivatized with *tert*-butyldimethylsilyl groups via reaction with *N*-methyl-*N*-(*tert*-butyldimethylsilyl)trifluoroacetamide and were subjected to GC/MS. The derivatized amino acids were identified by retention time, which was confirmed using a set of derivatized standards. The extent of labeling in the M-57 fragment was monitored. This fragmentation involves loss of a *t*-butyl radical and is quite facile; often the molecular ion was not observed. A number of amino acids were monitored for $^{13}$C labeling including aspartic acid, glutamic acid, alanine, glycine, valine, leucine, isoleucine, proline, methionine, serine, threonine, lysine, and phenylalanine. The amount of isotope incorporation was determined by comparison to a natural abundance MSP sample, which was subjected to the same procedure. All GC/MS analyses were done in triplicate.

*PSII Preparations*—PSII membranes were isolated from market spinach (43, 44). This material was treated to remove native MSP, as well as the 18- and 24-kDa extrinsic proteins, while retaining manganese (see method in Ref. 21 and references therein). Either natural abundance, globally $^{13}$C-, [$^{13}$C]Asp/Asn- or [$^{13}$C]Glu/Gln-labeled MSP was rebound to PSII according to established procedures (see Ref. 21 and references therein). These PSII membranes were used directly for FT-IR spectroscopy at 277 K and were in a sucrose buffer containing 0.4 M sucrose, 50 mM MES-NaOH, pH 6.0, 60 mM NaCl, and 20 mM CaCl$_2$. PSII complexes, for FT-IR spectroscopy at 200 K, were purified from the membranes via detergent solubilization and ion-exchange chromatography (45). The final buffer contained 25% glycerol, 50 mM MES-NaOH, pH 6.0, 0.05% lauryl maltoside, 7.5 mM CaCl$_2$, and 0.26 M NaCl.

Oxygen evolution assays were employed to verify reconstitution. The samples contained 10–15 μg/ml Chl, 20 mM calcium chloride, 0.33 mM recrystallized 2,6-dichloro-*p*-benzoquinone, 1 mM potassium ferricyanide, 50 mM MES-NaOH, pH 6.0, 60 mM NaCl, and 400 mM sucrose. A Clark-type O$_2$ electrode was employed (YSI 5300, YSI Inc., Yellow Springs, OH) (46). As isolated, the oxygen evolution rates for PSII membranes and PSII complexes were >750 and >1000 μmol of O$_2$ (mg of Chl·h)$^{-1}$, respectively. The oxygen evolution rates for all MSP reconstituted PSII membranes were between 250 and 500 μmol of O$_2$ (mg of Chl·h)$^{-1}$. This range of oxygen evolution rates is typical for this type of PSII sample (see Refs. 11, 21, 23, and 35 and references therein). The oxygen evolution rates for all MSP-reconstituted PSII complexes were indistinguishable and were between 400 and 600 μmol of O$_2$ (mg of Chl·h)$^{-1}$.

*FT-IR Spectroscopy at 200 K*—Infrared spectra at 200 K were recorded on a Nicolet 60-SXR FT-IR spectrometer equipped with a liquid nitrogen-cooled MCT/B detector and a KBr beamsplitter (25, 47). Data were recorded under 10 min of illumination, and 2500 mirror scans were added together for each double-sided interferogram. The mirror velocity was 1.57 cm s$^{-1}$, a Happ-Genzel apodization function was used, and the spectral resolution was 8 cm$^{-1}$. A PSII sample (3 μl) was placed on a 25-mm germanium window and was concentrated in the dark under a stream of nitrogen for 5 min at 4 °C. Each sample also contained 20 equivalents of potassium ferricyanide. The germanium window was sandwiched with a CaF$_2$ window and placed in the spectrometer. The sample was precooled to 200 K. Upon warming again to 277 K, the sample was preilluminated for 30 s and then allowed to reach the dark-adapted state over an additional 2 min. This procedure equalizes the contributions of the slowly decaying radical, $Y_D^\cdot$, and any slowly decaying $Chl_Z^+$ to each spectrum (48–50). The temperature control apparatus and illumination conditions have been described previously

(25, 47, 51). The temperature was continuously monitored and was $200 \pm 0.3$ K. Red and heat filters were employed. The amide I absorbance for each sample was between 0.2 and 0.6, and all spectra were normalized to an amide II absorbance of 0.5. The normalization corrects for differences in protein concentration and path length. Dark-minus-dark spectra were recorded before illumination at 200 K.

*FT-IR Spectroscopy at 277 K*—Infrared spectra at 277 K were recorded on a Bruker (Billerica, MA) IFS-66v/S FT-IR spectrometer equipped with a liquid nitrogen-cooled MCT detector and a Harrick (Ossining, NY) temperature controller (35, 36). A Happ-Genzel apodization function and four levels of zero filling were used. The spectral resolution was 8 cm$^{-1}$. Both the actinic and pre-flashes were provided by a frequency doubled, 532-nm output from a Surelight III Nd:YAG laser (Continuum, Santa Clara, CA). The pulse width was ~7 ns, and the pulse energy was 20–30 mJ cm$^{-2}$. A PSII sample (2 $\mu$l), containing 10 eq of ferricyanide and 2 eq of 2,6-dichloro-p-benzoquinone, was placed on a 25-mm CaF$_2$ window and was concentrated in the dark under a stream of nitrogen for 7 min at 4 °C. The window was sandwiched with another CaF$_2$ window, placed in the spectrometer, and cooled to 277 K. A germanium filter was used to block the light from the internal laser of the spectrometer. The sample was allowed to equilibrate for 30 min after which it was given a preflash. After an additional 60 min of dark adaptation, an actinic flash was applied, and 200 mirror scans (~30 s of data) were summed for each double-sided interferogram. The spectra taken after the flash were ratioed to data taken immediately before the flash. Dark-minus-dark spectra were recorded before each actinic flash. In each sample, the amide I absorbances were between 0.6 and 0.9, and each spectrum was normalized to an amide II absorbance of 0.5. A total of 18 data sets were collected for each sample type.

## RESULTS

*Isotopic Labeling*—To probe the role of acidic amino acid residues in MSP, aspartic acid/asparagine and glutamic acid/glutamine were selectively labeled. To accomplish this, a strain of *E. coli* (BL21/DE3), in which the expression of MSP had been previously optimized, was employed. Cultures were grown in defined media containing each essential amino acid, nucleotide, mineral, and vitamin. Ammonium chloride and glucose were employed as additional nitrogen and carbon sources, respectively. Labeled amino acids were present in the media throughout the growth of the culture and during MSP induction. Following purification (21, 40), MSP was hydrolyzed and derivatized. The derivatized amino acids were subjected to GC/MS analysis. Acid hydrolysis is expected to deaminate glutamine and asparagine, and the detection of Asn and Gln is difficult with this method (42). However, both Asn and Gln are expected to be labeled from $^{13}$C-labeled aspartate and glutamate, respectively (52). MSP was also globally labeled with $^{13}$C by methods previously described (21, 23).

The extent of $^{13}$C incorporation into 12 amino acids was monitored, and the results are presented in Table I. Culture supplementation with [$^{13}$C]aspartic acid (L-[4-$^{13}$C]aspartic acid) resulted in $^{13}$C labeling (65%) of Asp/Asn residues in MSP. Scrambling was not extensive, and involved only glutamic acid (7%), threonine (25%), and lysine (14%). Examination of the metabolic pathways in *E. coli* suggests that the label incorporated into threonine and lysine will be in the side chain (52). Arginine was difficult to detect in the gas chromatogram, but was observed in three experimental trials. In those experiments, no significant label (<1%) was detected in arginine (data not shown). No $^{13}$C labeling was detected in any other amino acids (Table I), indicating that $^{13}$C was not incorporated into the peptide backbone.

[$^{13}$C]Glutamate labeling is expected to be more difficult, when compared with aspartic acid labeling (39, 53). However, we found reasonable (41%) amounts of labeling from [$^{13}$C]glutamic acid (L-[5-$^{13}$C]glutamic acid) into Glu/Gln, with very little label scrambling. Of the examined amino acids, only Asp/Asn (9%) showed any evidence of significant $^{13}$C incorporation. The results in Table I indicate that although the glutamic acid label

TABLE I
*Isotopic labeling of MSP as determined with GC-MS*

All data were obtained from the *tert*-butyl dimethylsilyl derivatives of the amino acids, which were generated from MSP by anaerobic acid hydrolysis. The extent of labeling was determined from the M-57 peak, which represents the cation resulting from the loss of a *t*-butyl radical. Values, determined as the mean of three measurements, are reported as percent (%). The percent isotope incorporation was determined by comparison to a natural abundance sample. The standard deviation for each measurement was less than 1.0% of the mean.

| Amino acid | Global $^{13}$C$^a$ | [$^{13}$C]Asp$^b$ | [$^{13}$C]Glu$^b$ |
|---|---|---|---|
| Aspartic acid$^c$ | 91.7 | 65.1 | 9.3 |
| Glutamic acid$^d$ | 91.5 | 6.7 | 40.9 |
| Alanine | 91.9 | ND$^e$ | ND |
| Glycine | 91.2 | ND | ND |
| Valine | 92.0 | ND | ND |
| Leucine | 91.1 | ND | ND |
| Isoleucine | 87.4 | ND | ND |
| Proline | 91.4 | ND | ND |
| Methionine | 92.6 | ND | 1.4 |
| Serine | 90.9 | ND | ND |
| Threonine | 91.6 | 25.1 | ND |
| Lysine | 89.0 | 13.7 | ND |
| Phenylalanine | 92.2 | ND | ND |

$^a$ Extent of uniform $^{13}$C labeling.
$^b$ Extent of $^{13}$C labeling at one carbon atom.
$^c$ Aspartic acid and deamidated asparagine.
$^d$ Glutamic acid and deamidated glutamine.
$^e$ ND, labeling in these amino acids was not detected (<1%).

was diluted, the $^{13}$C isotope was not significantly incorporated into other amino acids.

When MSP was expressed in minimal media containing [$^{13}$C]glucose, all amino acids were labeled, with an average $^{13}$C isotopic enrichment of 91% (Table I). This result is in agreement with an earlier report (21).

*Infrared Spectroscopy at 200 K*—Selectively labeled MSP was reconstituted to PSII, and these PSII samples were used for difference FT-IR spectroscopy at 200 K. At 200 K it has been shown that continuous illumination can be used to generate a $S_2Q_A^-$-minus-$S_1Q_A$ spectrum (see Ref. 25 and references therein). The data in Fig. 1, *A–C*, represent $S_2Q_A^-$-minus-$S_1Q_A$ difference spectra acquired from PSII samples containing natural abundance, [$^{13}$C]Glu/Gln-, or [$^{13}$C]Asp/Asn-labeled MSP, respectively. The $^{12}$C MSP spectrum is similar to data obtained previously at this temperature (25, 29, 47, 51). Because all the spectra were corrected for path length and concentration, they were directly subtracted on a one to one basis, to generate the isotope-edited spectrum (Figs. 2 and 3). Photooxidation-induced changes in MSP are the only expected contributors to the isotope-edited spectrum; this spectrum will exhibit isotope shifts caused by $^{13}$C labeling of amino acid residues. Fig. 1*D* represents a control dark-minus-dark spectrum.

As observed in Figs. 2 and 3, the isotope-edited spectra exhibit isotope-induced shifts in vibrational bands, which are above the noise in the measurement. The level of the noise was assessed by comparison to a control double difference spectrum (Figs. 2*C* and 3*C*), constructed by subtraction of one-half of a data set from the other half of that same set. The data in *A* and *B* (Figs. 2 and 3) were acquired from [$^{13}$C]Glu/Gln- and [$^{13}$C]Asp/Asn-labeled MSP samples, respectively. The spectra have several features in common. These features include derivative-shaped bands in the 1678–1643, 1562–1551, and 1265–1250 cm$^{-1}$ spectral regions.

Possible contributors in these three regions are the amide I, II, and III bands, arising from C = O and CN/NH vibrations of the peptide backbone (54). However, GC/MS indicated that there was no $^{13}$C incorporation into the peptide backbone (Table I). Therefore, we do not favor peptide backbone-derived amide I, II, or III assignments for these bands.
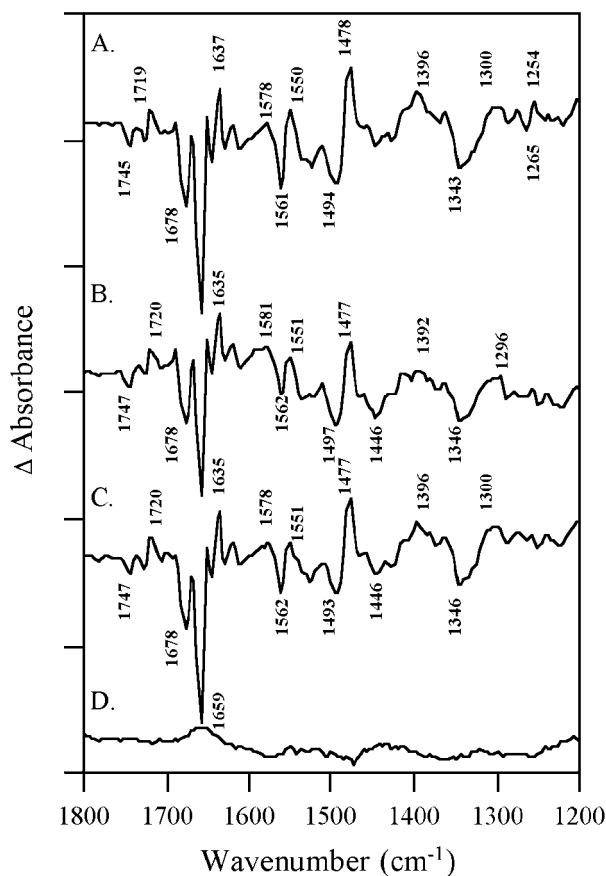
Fig. 1. **$S_2Q_A^-$-minus-$S_1Q_A$ FT-IR spectra obtained at 200 K under continuous illumination.** Spectra **A**, **B**, and **C** represent the light-minus-dark difference FT-IR spectra of reconstituted PSII samples containing natural abundance, [13C]Glu/Gln-, and [13C]Asp/Asn MSP, respectively. Spectrum **D** is a representative dark-minus-dark spectrum. The spectra in **A** and **C** are averages of 14 data sets, whereas the spectrum in **B** is the average of 10 data sets. The *tick marks* on the y axis represent 0.0005 absorbance units.



Fig. 2. **The 1800–1500 cm$^{-1}$ region of isotope-edited, double difference spectra acquired at 200 K.** Spectrum **A** shows the effect of [13C]Gln/Glu labeling and was constructed by the direct subtraction of Fig. 1, *B* from *A*. Spectrum **B** shows the effect of [13C]Asn/Asp labeling and was constructed by the direct subtraction of Fig. 1, *C* from *A*. Spectrum **C** is a representative control double difference spectrum, in which no spectral contributions are expected. **C** was constructed from the data shown in Fig. 1*B* and gives an estimate of the noise in the measurement. The data in **C** were corrected for the difference in data acquisition time when *C* is compared with *A* or *B*. The *tick marks* on the y axis represent 0.0002 absorbance units.

When the MSP-expressing strain was cultured in [13C]glutamic acid (Figs. 2*A* and 3*A*), GC/MS showed that only the Glu/Gln (41%) and Asp/Asn (9%) side chains of MSP were significantly labeled. When the MSP-expressing strain was cultured in [13C]aspartic acid (Figs. 2*B* and 3*B*), GC/MS showed that Asp/Asn (65%), Glu/Gln (7%), lysine (14%), and threonine (25%) were labeled. Labeling of the threonine or lysine side chain from aspartate would not result in spectral contributions in the amide I, II, and III regions and is also not observed in [13C]Asp-labeled samples (Table I). Therefore, the bands in common, when Figs. 2*A* and 3*A* are compared with Figs. 2*B* and 3*B*, are assigned to the amide I, II, and III vibrations of glutamine and asparagine side chains, which are labeled in both samples and are the only amino acid side chains to contain an amide group.

The frequencies of the amide I, II, and III vibrations of the glutamine side chain in polar solutions are observed and/or calculated to be 1654, 1595, 1271 cm$^{-1}$, respectively (55), in reasonable agreement with the frequencies observed in our isotope-edited spectrum (Figs. 2*A* and 3*A*). An isotope shift is to be expected for each normal coordinate because the C = O carbon of the side chain is the labeled atom. To be consistent with the observed intensities, a glutamine contribution must occur in Figs. 2*A* and 3*A*, and an asparagine contribution must occur (with similar frequencies) in Figs. 2*B* and 3*B*. The observed, derivative-shaped bands are consistent with a change in the environment of these residues upon photooxidation of
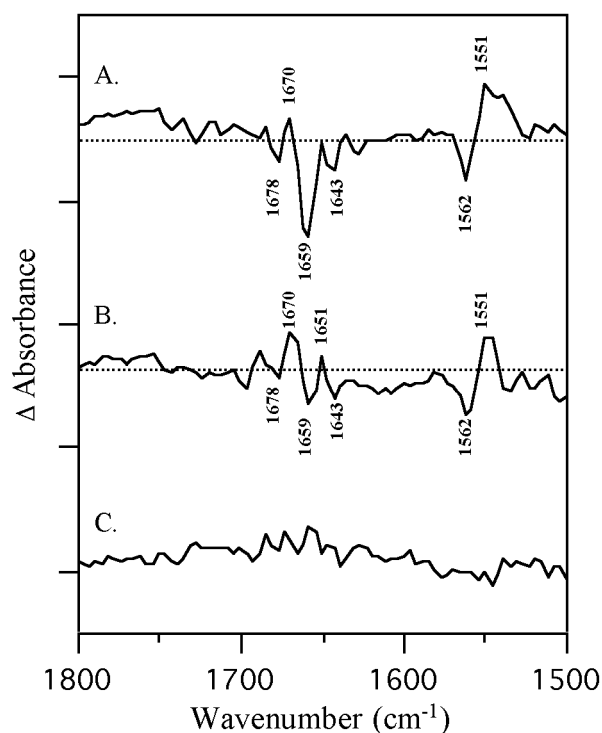
manganese. Possible environmental changes include a change in polarity, hydrogen bonding, or electric field when manganese is oxidized.

Additional features are observed in the isotope-edited data acquired from [13C]Glu/Gln-labeled MSP (Figs. 2*A* and 3*A*). Broad positive and negative spectral contributions are observed between 1477 and 1323 cm$^{-1}$. In this region, these data show some similarity to data previously obtained at 200 K with globally 13C-labeled MSP (23). These bands were attributed previously to the symmetric stretching vibrations of deprotonated aspartic or glutamic acid residues in MSP. Small alterations in frequency, as observed when these data are compared with the earlier report, could be because of small contributions from the methylene bending modes of glutamine, which also make a contribution in this spectral region and which may be weakly 13C = O isotope-sensitive (55). The appearance of isotope shifts in the 1477–1323 cm$^{-1}$ region of the [13C]Glu/Gln-labeled data suggests that these bands may arise from the symmetric stretching vibration of a deprotonated glutamate side chain. However, other spectral features, previously assigned to the asymmetric stretching vibration of glutamate and the C = O carbonyl stretching vibration of glutamic acid are not observed (23). This may be because of the decrease in 13C labeling efficiency (from ~90 to 40%) and the weaker (more than a factor of 2) intrinsic infrared intensity of these bands. Thus, these data suggest that a glutamic acid in MSP deprotonates at this temperature. Weak spectral features in the 1477–1323 cm$^{-1}$ region of Fig. 3*B* may be due to the low amount of label scrambling from Asp to Glu in the [13C]Asp/Asn-labeled samples (Table I).

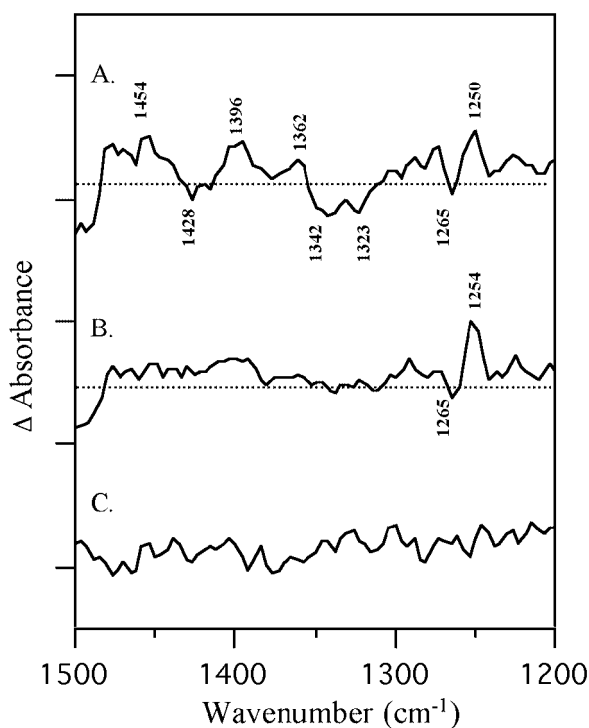FIG. 3. **The 1500–1200 cm$^{-1}$ region of isotope-edited, double difference spectra acquired at 200 K.** Spectrum **A** shows the effect of [$^{13}$C]Gln/Glu labeling and was constructed by the direct subtraction of Fig. 1, *B* from *A*. Spectrum **B** shows the effect of [$^{13}$C]Asn/Asp labeling and was constructed by the direct subtraction of Fig. 1, *C* from *A*. Spectrum **C** is a representative control double difference spectrum, in which no spectral contributions are expected. **C** was constructed from the data shown in Fig. 1*B* and gives an estimate of the noise in the measurement. The data in **C** were corrected for the difference in data acquisition time when C is compared with *A* or *B*. The *tick marks* on the *y* axis represent 0.0002 absorbance unit.

*Infrared Spectroscopy at 277 K*—PSII samples, reconstituted with labeled MSP, were irradiated with a single laser flash and examined at 277 K. In these FT-IR experiments, a $S_2Q_B^-$-minus-$S_1Q_B$ spectrum is acquired (35–37). The spectra shown in Fig. 4, *A–D*, represent $S_2Q_B^-$-minus-$S_1Q_B$ difference spectra acquired from PSII samples containing natural abundance, globally [$^{13}$C]-, [$^{13}$C]Glu/Gln-, or [$^{13}$C]Asp/Asn-MSP, respectively. The natural abundance spectrum (Fig. 4*A*) is similar to $S_2Q_B^-$-minus-$S_1Q_B$ data reported previously (32, 33, 35–37). Fig. 4*E* represents a dark-minus-dark spectrum.

Because the spectra were corrected for path length and concentration, they can be directly subtracted on a one to one basis, to generate the isotope-edited spectrum. The isotope-edited data in Fig. 5, *A–C*, were acquired from globally [$^{13}$C]-, [$^{13}$C]Glu/Gln- and [$^{13}$C]Asp/Asn-labeled MSP samples, respectively. Given the signal to noise ratio (see control double difference, Fig. 5*E*), the data have one spectral feature in common. This common spectral feature is a positive band at 1632–1634 cm$^{-1}$. Because of the frequency, we assign this positive band to a [$^{13}$C]glutamine contribution in the [$^{13}$C]Glu/Gln sample (Fig. 5*B*) and a [$^{13}$C]asparagine contribution in the [$^{13}$C]Asp/Asn-labeled sample (Fig. 5*C*). This positive band is most likely the isotopically shifted $^{13}$C isotopomer band, with the corresponding negative $^{12}$C band found in the 1650 cm$^{-1}$ region, which is not interpretable in these data. This spectral feature may arise from a change in polarity, hydrogen bonding, or electrostatics, which is in turn because of photooxidation of manganese at 277 K.

When MSP is globally $^{13}$C-labeled (Fig. 5*A*), this Asn/Gln band is also observed in the 1632–1634 cm$^{-1}$ region, as ex-
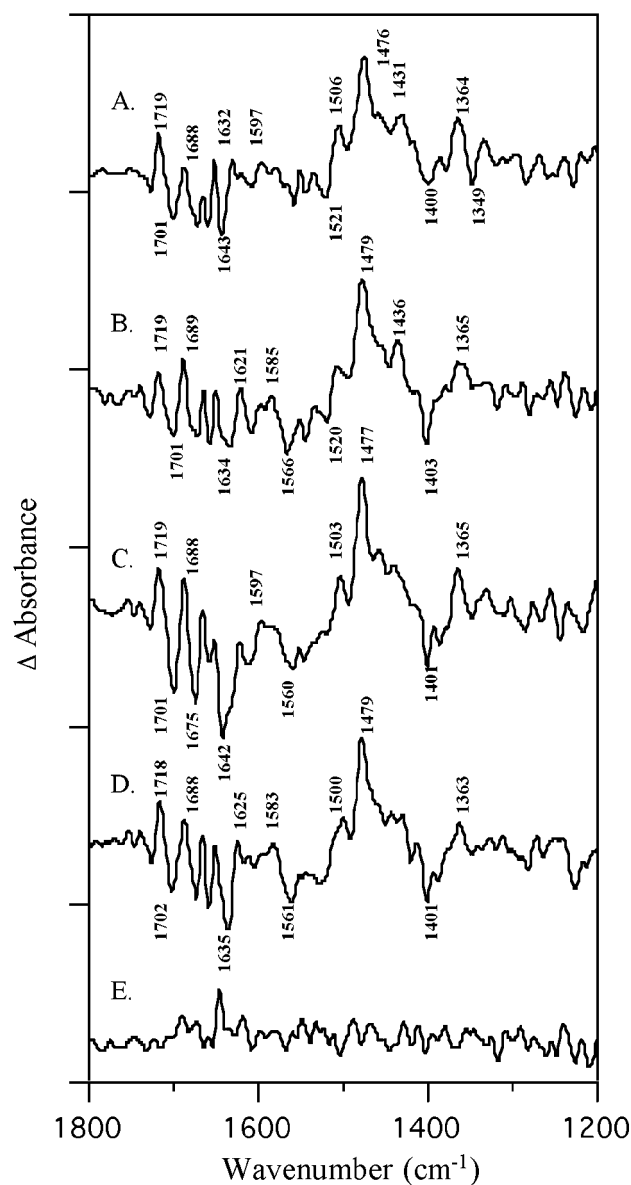


FIG. 4. **$S_2Q_B^-$-minus-$S_1Q_B$ FT-IR spectra obtained at 277 K after a single laser flash.** Spectra **A**, **B**, **C**, and **D** represent the light-minus-dark difference FT-IR spectra of reconstituted PSII samples containing natural abundance, globally $^{13}$C-, [$^{13}$C]Glu/Gln-, and [$^{13}$C]Asp/Asn-labeled MSP, respectively. Spectrum **E** is a representative dark-minus-dark spectrum. All spectra are averages of 18 different data sets. The *tick marks* on the *y* axis represent 0.0002 absorbance units.

pected (Table I). However, the intensity of this band does not scale with the increase in the amount of Asn/Gln labeling in the globally $^{13}$C-labeled sample. This can be seen by comparison of the globally $^{13}$C-labeled data (Fig. 5*A*) with the result of averaging the [$^{13}$C]Glu/Gln and [$^{13}$C]Asp/Asn labeled data (Fig. 5*D*). This discrepancy in the intensities may be caused by overlapping additional negative contribution in the globally $^{13}$C-labeled sample, in which all amino acid side chains and the peptide bond are labeled. Note that Asn and Gln contributions are identified both in our 200 K (Figs. 2 and 3) and our 277 K data (Fig. 5), but the observed spectral frequencies are different at the two temperatures (see "Discussion" below).

The only other spectral features above the noise in the 277 K measurements are observed in the 1700–1677 cm$^{-1}$ region of the [$^{13}$C]Glu/Gln-labeled sample (Fig. 5*B*). In this sample, the amino acids labeled are mainly Glu/Gln, with only a small amount of label scrambling into Asp/Asn. Therefore, we assign
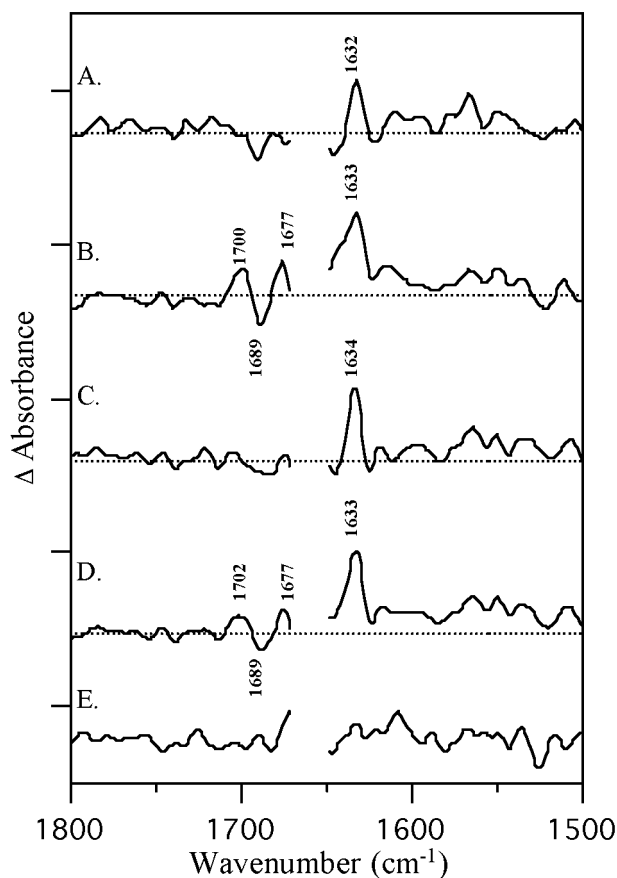
FIG. 5. **The 1800–1500 cm$^{-1}$ region of the isotope-edited, double difference spectra acquired at 277 K.** Spectrum **A** shows the effect of $^{13}$C global labeling, and was constructed by direct subtraction of Fig. 4, *B* from *A*. Spectrum **B** shows the effect of [$^{13}$C]Gln/Glu labeling and was constructed by the direct subtraction of Fig. 4, *C* from *A*. Spectrum **C** shows the effect of [$^{13}$C]Asn/Asp labeling and was constructed by the direct subtraction of Fig. 4, *D* from *A*. Spectrum **D** is the average of **B** and **C**. Spectrum **E** is a representative control double difference spectrum, in which no spectral contributions are expected. **E** was constructed from the data shown in Fig. 4*A* and gives an estimate of the noise in the measurement. The data in **E** were corrected for the difference in data acquisition time. Note that the region between 1670 and 1650 cm$^{-1}$ is not interpretable, because of the presence of a small spectral artifact in this region in the control spectrum (*E*). The *tick marks* on the *y* axis represent 0.0002 absorbance units.

the (+) 1700, (−) 1689, and (+) 1677 cm$^{-1}$ bands in Fig. 5*B* to Glu/Gln. The frequencies suggest an assignment to the C = O stretch of a glutamate with an elevated p$K_a$, which can result from a hydrophobic environment or from the presence of negative charges in the vicinity of the glutamate (for an example, see Ref. 56). Whereas these bands are still above the noise in the [$^{13}$C]Glu/Gln and [$^{13}$C]Asp/Asn averaged spectrum (Fig. 5*D*), they are not observed with significant intensity in the globally $^{13}$C-labeled case (Fig. 5*A*). This result again suggests cancellation effects in Fig. 5*A*, caused by more complex contributions to the isotope-edited data, when all amino acids and the peptide bond are labeled. The pattern of positive, negative, and positive bands in Fig. 5*B* can result from an isotope shift of a derivative-shaped band. Thus, Fig. 5*B* suggests that photooxidation of manganese perturbs the vibrational frequency of a glutamic acid C = O in MSP. Note that the 200 K data (Figs. 2 and 3) also were consistent with a perturbation to a glutamate, but that the frequencies and, therefore, the mechanism of the perturbation appears to be different at the two temperatures, with a possible deprotonation reaction occurring at 200 K and a polarity, electrostatic, or hydrogen bonding shift occurring at 277 K.

*FT-IR Spectroscopy at 277 K with DCMU*—277 K experiments were also performed with PSII samples, to which DCMU had been added. DCMU is an inhibitor that blocks electron transfer to $Q_B$ (57, 58). Thus, in the presence of DCMU, a single laser flash produces a $S_2Q_A^-$-minus-$S_1Q_A$ spectrum. MSP was natural abundance or globally $^{13}$C-labeled. The isotope-edited spectra acquired in the presence of DCMU were similar to the isotope-edited spectrum shown in Fig. 5*A* (data not shown).

DISCUSSION

In this report, we describe a method to label Asp/Asn and Glu/Gln residues in MSP. There are two primary concerns when attempting to label specific amino acids in a bacterially expressed protein. The first is that the label will be diluted via amino acid biosynthesis from other carbon and nitrogen sources in the media. The second is the possibility that the label will scramble to other amino acids via direct conversion of one amino acid into another (59). As this work shows, label scrambling can be mitigated by supplying high concentrations of amino acids to inhibit native amino acid biosynthesis. Aspartic acid is a direct precursor in the biosynthesis of asparagine, methionine, threonine, and lysine (52). In our work, significant scrambling of the label was only observed into threonine and lysine (see Table I). Glutamate is the direct precursor of glutamine, proline, and arginine (52). Glutamate also plays a pivotal role in amino acid synthesis via transamination reactions. This makes the labeling of this amino acid in high yield challenging (59). We attribute the less efficient labeling of this amino acid (41%), as compared with aspartic acid (65%), to this complex role of glutamate in metabolism.

In our experiments, difference FT-IR spectra were acquired at two different temperatures, and perturbations of Glu, Gln, and Asn side chains in MSP were observed under both sets of conditions. Whereas many spectral features are in common, when the 200 K and the 277 K spectra are compared, the 200 and 277 K spectra show some dissimilarity in the 1500–1200 cm$^{-1}$ region. The origin of these spectral differences has been discussed previously (35, 36). Assignments of the 200 K spectra, based on global isotopic labeling and site-directed mutagenesis, have been described (25, 29, 47, 51). In particular, at 200 K, our previous isotope editing work has shown that a subset of the carboxylates, contributing to the spectra, is on MSP (23). Assignments of the 277 K spectrum, based on global isotopic labeling in cyanobacterial PSII, have also been presented (33). Our aim in this work was to identify the subset of spectral contributions arising from Asp/Asn and Glu/Gln residues on MSP.

Using specifically labeled MSP, we have observed that photooxidation of manganese during the $S_1$ to $S_2$ transition perturbs asparagine, glutamine, and glutamate residues in this PSII subunit. Thus, conformational changes in MSP may be thermodynamically linked to at least one of the S state transitions. Thermodynamically linked structural changes have the potential to participate in a reaction mechanism by alteration of the free energy for the reaction. As an example of a possible perturbative mechanism, selected Asn and Gln side chains may participate in a hydrogen bonding network, which is perturbed upon manganese photooxidation. Oxidation of manganese may also generate an electric field or a change in polarity (by allowing or preventing the access of water), and either of these two effects may also be the origin of the perturbation.

As mentioned above, both at 200 and 277 K, frequency perturbations of Asn and Gln residues in MSP were observed. However, the observed frequencies of the Asn and Gln contributions were different at the two temperatures. Both at 200 and 277 K, a Glu contribution is observed. However, at 277 K, the spectral signature suggests a perturbative effect, while, at

200 K, the spectral signature may be more consistent with a glutamic acid deprotonation reaction. We can explain these temperature-related differences in frequency, because the 200 K data are obtained under conditions in which the enzyme is inhibited in oxygen evolution. At this temperature only the $S_1$ to $S_2$ transition can occur, and the other S state transitions are blocked (60). This inhibitory effect may be related to inhibition of a donor-side protonation reaction. Therefore, one possible explanation of our results is that MSP is involved in a proton transfer reaction, in which a MSP Glu is a participant. In this speculative model, a Glu side chain on MSP releases a proton when manganese is photooxidized and then is reprotonated, perhaps from solvent. In the context of this speculative model, the 200 K results can be explained by proposing that at low temperatures an intermediate is trapped, in which the Glu side chain has been deprotonated, but in which the reprotonation is blocked. Such an inhibition of a protonation reaction could lead to differences in electrostatics and hydrogen bonding, which in turn could cause the observed changes in the frequency of the Asn and Gln amide I, II, and III vibrations.

There are 14 Asp, 21 Glu, 11 Gln, and 7 Asn encoded in the sequence of processed spinach MSP (61). Mutations, deletions, and cross-linking have been used previously to probe the structure and function of amino acid residues in MSP (reviewed in Ref. 62). Secondary and tertiary structural modeling have been described (63–65), and preliminary assignments of MSP electron density in cyanobacterial PSII crystals have been reported at low resolution (4, 5). Residues at the $NH_2$-terminal end have been identified as critical for PSII binding (66–70), as have residues at the COOH terminus (14, 71). Regions of MSP that block PSII binding, when labeled (72), are possible candidates to contain some of the perturbed MSP residues observed here. These regions are the carboxyl terminus ($Glu^{212}$-$Gln^{247}$) and the region from $Asp^{157}$ to $Asp^{168}$ (72). The carboxyl-terminal region is particularly rich in both glutamate and glutamine (61).

The fact that the asparagine and glutamine frequencies are similar to each other is of interest. Both amino acid side chains contain an amide bond, but, ordinarily, one would expect that the microenvironment of the side chain would influence the frequency and that frequency differences would be observed when the side chains are in different protein environments. Similar frequencies suggest that the local environments of perturbed Asn and Gln residues are similar and that these residues are close together in the primary sequence or in the final tertiary structure of MSP. The sequence of spinach MSP reveals one dipeptide, QN, at positions 73 and 74 (61). This interesting part of the protein is in a region of the protein predicted to participate in a $\beta$ sheet structural element (63).

MSP alters the rate of the S state transitions and also enhances the stability of the manganese cluster (reviewed in Ref. 7). Our work suggests that Asn, Gln, and Glu residues on MSP are perturbed by hydrogen bonding, electric field, or polarity changes during the $S_1$ to $S_2$ transition. Proton transfer, involving one or more MSP Glu residues, may also be relevant to the mechanism of water oxidation, and low temperatures may trap an intermediate in a proton transfer reaction. In future experiments, we will examine changes in MSP during the other S state transitions.

## REFERENCES

1. Britt, R. D. (1996) in *Oxygenic Photosynthesis: The Light Reactions* (Ort, D. R., and Yocum, C. F., eds) Vol. 4, pp. 137–164, Kluwer Academic Publisher, Dordrecht
2. Bricker, T. M., and Frankel, L. K. (2002) *Photosyn. Res.* **72,** 131–146
3. Nanba, O., and Satoh, K. (1987) *Proc. Natl. Acad. Sci. U. S. A.* **84,** 109–112
4. Zouni, A., Witt, H.-T., Kern, J., Fromme, P., Krauss, N., Saenger, W., and Orth, P. (2001) *Nature* **409,** 739–743
5. Kamiya, N., and Shen, J.-R. (2003) *Proc. Natl. Acad. Sci. U. S. A.* **100,** 98–103
6. Joliot, P., and Kok, B. (1975) in *Bioenergetics of Photosynthesis* (Govindjee, ed) pp. 388–412, Academic Press, New York
7. Seidler, A. (1996) *Biochim. Biophys. Acta* **1277,** 35–60
8. Ono, T., and Inoue, Y. (1983) *FEBS Lett.* **164,** 252–260
9. Miyao, M., and Murata, N. (1983) *FEBS Lett.* **164,** 375–378
10. Miyao, M., and Murata, N. (1984) *FEBS Lett.* **170,** 350–354
11. Bricker, T. M. (1992) *Biochemistry* **31,** 4623–4628
12. Seidler, A., and Michel, H. (1990) *EMBO* **9,** 1743–1748
13. Betts, S. D., Ross, J. R., Hall, K. U., Pichersky, E., and Yocum, C. F. (1996) *Biochim. Biophys. Acta* **1274,** 135–142
14. Lydakis-Simantiris, N., Betts, S. D., and Yocum, C. (1999) *Biochemistry* **38,** 15528–15535
15. Zubrzycki, I. Z., Frankel, L. K., Russo, P. S., and Bricker, T. M. (1998) *Biochemistry* **37,** 13553–13558
16. Svensson, B., Tiede, D. M., and Barry, B. A. (2002) *J. Phys. Chem. B* **106,** 8485–8488
17. Xu, Q., Nelson, J., and Bricker, T. M. (1994) *Biochim. Biophys. Acta* **1188,** 427–431
18. Shutova, T., Irrgang, K.-D., Shubin, V., Klimov, V. V., and Renger, G. (1997) *Biochemistry* **36,** 6350–6358
19. Lydakis-Simantiris, N., Hutchison, R. S., Betts, S. D., Barry, B. A., and Yocum, C. F. (1999) *Biochemistry* **38,** 404–414
20. Ahmed, A., Tajmir-Riahi, H. A., and Carpentier, R. (1995) *FEBS Lett.* **363,** 65–68
21. Hutchison, R. S., Betts, S. D., Yocum, C. F., and Barry, B. A. (1998) *Biochemistry* **37,** 5643–5653
22. Tohri, A., Suzuki, T., Okuyama, S., Kamino, K., Motoki, A., Hirano, M., Ohta, H., Shen, J.-R., Yamamoto, Y., and Enami, I. (2002) *Plant Cell Physiol.* **43,** 429–439
23. Hutchison, R. S., Steenhuis, J. J., Yocum, C. F., Razeghifard, R. M., and Barry, B. A. (1999) *J. Biol. Chem.* **274,** 31987–31995
24. Enami, I., Kamo, M., Ohta, H., Takahashi, S., Miura, T., Kusayanagi, M., Tanabe, S., Kamei, A., Motoki, A., Hirano, M., Tomo, T., and Satoh, K. (1998) *J. Biol. Chem.* **273,** 4629–4634
25. Steenhuis, J. J., and Barry, B. A. (1997) *J. Phys. Chem.* **101,** 6652–6660
26. Dismukes, G. C., and Siderer, Y. (1981) *Proc. Natl. Acad. Sci. U. S. A.* **78,** 274–278
27. de Paula, J. C., Innes, J. B., and Brudvig, G. W. (1985) *Biochemistry* **24,** 8114–8120
28. Roelofs, T. A., Liang, W., Latimer, M. L., Cinco, R. M., Rompel, A., Andrews, J. C., Sauer, K., Yachandra, V. K., and Klein, M. P. (1996) *Proc. Natl. Acad. Sci. U. S. A.* **93,** 3335–3340
29. Steenhuis, J. J., Hutchison, R. S., and Barry, B. A. (1999) *J. Biol. Chem.* **274,** 14609–14616
30. Noguchi, T., Ono, T.-A., and Inoue, Y. (1995) *Biochim. Biophys. Acta* **1232,** 65–66
31. Noguchi, T., Tomo, T., and Kato, C. (2001) *Biochemistry* **40,** 1497–1502
32. Hillier, W., and Babcock, G. (2001) *Biochemistry* **40,** 1503–1509
33. Noguchi, T., and Sugiura, M. (2003) *Biochemistry* **42,** 6035–6042
34. Barry, B. A. (2000) *Photosyn. Res.* **65,** 197–198
35. Halverson, K. M., and Barry, B. A. (2003) *Biophys. J.* **85,** 1317–1325
36. Halverson, K. M., and Barry, B. A. (2003) *Biophys. J.* **85,** 2581–2588
37. Zhang, H., Fischer, G., and Wydrzynski, T. (1998) *Biochemistry* **37,** 5511–5517
38. Griffey, R. H., Redfield, A. G., Loomis, R. E., and Dahlquist, F. W. (1985) *Biochemistry* **24,** 817–822
39. Ramesh, V., Frederick, R. O., Syed, S. E. H., Gibson, C. F., Yang, J., and Roberts, G. C. K. (1994) *Eur. J. Biochem.* **225,** 601–608
40. Betts, S. D., Hachigian, T. M., Pichersky, E., and Yocum, C. F. (1994) *Plant Mol. Biol.* **26,** 117–130
41. Kitson, F. G., Larsen, B. S., and McEwen, C. N. (1996) *Gas Chromatography and Mass Spectrometry, A Practical Guide*, Academic Press, San Diego
42. Patterson, B. W., Carraro, F., and Wolfe, R. R. (1993) *Biol. Mass Spectrom.* **22,** 518–523
43. Berthold, D. A., Babcock, G. T., and Yocum, C. F. (1981) *FEBS Lett.* **134,** 231–234
44. Anderson, L. B., Ouellette, A. J. A., and Barry, B. A. (2000) *J. Biol. Chem.* **275,** 4920–4927
45. MacDonald, G. M., and Barry, B. A. (1992) *Biochemistry* **31,** 9848–9856
46. Barry, B. A. (1995) *Methods Enzymol.* **258,** 303–319
47. Steenhuis, J. J., and Barry, B. A. (1996) *J. Am. Chem. Soc.* **118,** 11927–11932
48. MacDonald, G. M., Bixby, K. A., and Barry, B. A. (1993) *Proc. Natl. Acad. Sci. U. S. A.* **90,** 11024–11028
49. MacDonald, G. M., Steenhuis, J. J., and Barry, B. A. (1995) *J. Biol. Chem.* **270,** 8420–8428
50. Kim, S., and Barry, B. A. (1998) *Biophys. J.* **74,** 2588–2600
51. Steenhuis, J. J., and Barry, B. A. (1998) *J. Phys. Chem.* **102,** 4–8
52. Arnstein, H. R. V. (ed) (1978) *Amino Acid and Protein Biosynthesis II, International Review of Biochemistry*, Vol. 18, University Park Press, Baltimore
53. Muchmore, D. C., McIntosh, L. P., Russell, C. B., Anderson, D. E., and Frederick, W. D. (1989) *Methods Enzymol.* **177,** 44–73
54. Krimm, S., and Bandekar, J. (1986) in *Advances in Protein Chemistry* (Anfinsen, C. B., Edsall, J. T., and Richards, F. M., eds) Vol. 38, pp. 181–364, Academic Press, New York
55. Ramírez, F. L., Tuñón, I., and Silla, E. (1998) *J. Phys. Chem. B* **102,** 6290–6298
56. Wilson, N. A., Barbar, E., Fuchs, J. A., and Woodward, C. (1995) *Biochemistry* **34,** 8931–8939
57. Oettmeier, W., and Soll, H. J. (1983) *Biochim. Biophys. Acta* **724,** 287–290
58. Farineau, J., and Mathis, P. (1985) *Biochim. Biophys. Acta* **808,** 103–111
59. Waugh, D. (1996) *J. Biomol. NMR* **8,** 184–192
60. Styring, S., and Rutherford, A. W. (1988) *Biochim. Biophys. Acta* **933,** 378–387

61. Oh-oka, H., Tanaka, S., Wada, K., Kuwabara, T., and Murata, N. (1986) *FEBS Lett.* **197,** 63–66
62. Popelkova, H., Wyman, A., and Yocum, C. (2003) *Photosyn. Res.,* **77,** 21–34
63. Bricker, T., and Frankel, L. (1998) *Photosyn. Res.* **56,** 157–173
64. de las Rivas, J., and Heredia, P. (1999) *Photosyn. Res.* **1999,** 11–21
65. Pazos, F., Heredia, P., Valencia, A., and de las Rivas, J. (2001) *Proteins* **45,** 372–381
66. Eaton-Rye, J. J., and Murata, N. (1989) *Biochim. Biophys. Acta* **977,** 219–226
67. Odom, W. R., and Bricker, T. M. (1992) *Biochemistry* **31,** 5616–5620
68. Popelkova, H., Im, M. M., and Yocum, C. F. (2002) *Biochemistry* **41,** 10038–10045
69. Popelkova, H., Im, M. M., D'Auria, J., Betts, S. D., Lydakis-Simantiris, N., and Yocum, C. F. (2002) *Biochemistry* **41,** 2702–2711
70. Popelkova, H., Im, M. M., and Yocum, C. F. (2003) *Biochemistry* **42,** 6193–6200
71. Betts, S. D., Lydakis-Simantiris, N., Ross, J. R., and Yocum, C. F. (1998) *Biochemistry* **37,** 14230–14236
72. Frankel, L. K., Cruz, J. A., and Bricker, T. M. (1999) *Biochemistry* **38,** 14271–14278

# Specific Isotopic Labeling and Photooxidation-linked Structural Changes in the Manganese-stabilizing Subunit of Photosystem II

Roseann K. Sachs, Kelly M. Halverson and Bridgette A. Barry

---

Access the most updated version of this article at doi: 10.1074/jbc.M307148200

Alerts:
- When this article is cited
- When a correction for this article is posted

Click here to choose from all of JBC's e-mail alerts

This article cites 69 references, 10 of which can be accessed free at
http://www.jbc.org/content/278/45/44222.full.html#ref-list-1